Title

Investigating Potential Neuroprotective Effects of Montelukast, a Cysteinyl Leukotriene Receptor-1 Antagonist, in Neuro-HIV-presenting gp120 Mice

Author

Ortega, Maxine

Publication Date

2023

Peer reviewed|Thesis/dissertation

UNIVERSITY OF CALIFORNIA
RIVERSIDE

Investigating Potential Neuroprotective Effects of Montelukast, a Cysteinyl Leukotriene Receptor-1 Antagonist, in Neuro-HIV-presenting gp120 Mice

A Thesis submitted with partial satisfaction
of the requirements for the degree of

Master of Science

in

Biomedical Sciences

by

Maxine G. Ortega

December 2023

Thesis Committee:

Dr. Marcus Kaul, Chairperson
Dr. Emma Wilson
Dr. Todd Fiacco
Dr. Iryna Ethell

The Thesis of Maxine Ortega is approved:

_____

_____

_____

Committee Chairperson

University of California, Riverside

ACKNOWLEDGEMENTS

I would to thank my Principal Investigator, Dr. Marcus Kaul, for taking a chance on a program's only student-athlete and allowing me to be a member of your lab. Thank you for your flexibility and patience as I navigated my way through a Master's program and the NCAA Division 1 competition. I would have never been able to achieve both of these accomplishments without your part in my journey.

I would also like to thank the members of the Kaul lab, especially our lab manager, Ricky Maung, who guided me through all my experiments and analysis to generate this research and thesis that I have today. All of the Kaul lab members have each played a role in my research from answering all of the questions to assisting me with my harvest. I would not be the researcher I am today without all of you.

Lastly, I want to thank my family and friends who have supported and encouraged me to pursue my goals of higher education. You are my rock and this achievement belongs to us all.

ABSTRACT OF THE THESIS

The Neuroprotective Effects of Montelukast, a Cysteinyl Leukotriene Receptor-1 Antagonist, in Neuro-HIV-presenting gp120 Mice

by

Maxine Ortega

Master of Science, Graduate Program in Biomedical Sciences
University of California, Riverside, December 2023
Dr. Marcus Kaul, Chairperson

Antiretroviral therapy (ART) has played a key role in extending the longevity of individuals infected with HIV. Although life expectancy increased significantly, aging with the virus has presented a new study of interest as neurocognitive impairments begin manifestations in individuals living with HIV. These manifestations lead researchers to investigate the involvement of HIV and HIV-associated neurodegeneration (HAND). As interest in this area grows, researchers demonstrate the current pathology of neuro-HIV and the damage manifests in HAND patients. The current neuropathology of HIV neuronal damage demonstrates the initiation of CD4 and chemokine coreceptors, CCR5 and CXCR4 in the brain to activate macrophages and microglia for the release of neurotoxic substances to neurons. The use of ART has provided a decreased incidence of extreme neurological impairments in HIV patients, yet, there were no significant changes to the overall incidence of HAND with ART, producing a gap for treatment against neuro-HIV. Many researchers are currently investigating different targets in neuro-HIV pathogenesis, such as chemokines, cytokines, leukotrienes, etc., to inhibit inflammatory responses that could be used as potential treatments for neuroprotection. Montelukast is a

cysteinyl-leukotriene receptor 1 antagonist, initially used as an anti-inflammatory drug for asthma. Cysteinyl leukotrienes have been shown to correlate with the inflammatory response of neuro-HIV, which is why we want to see if the drug will inhibit this response and demonstrate neuroprotection in HIV-infected brains. In this paper, we will investigate the effects of a cysteinyl leukotriene receptor 1 antagonist, Montelukast in HIV gp120 mice We will conduct a 2-month administration of Montelukast and saline to HIV-gp120 transgenic and wild-type mice and then analyze the effects of the Montelukast through immunofluorescence staining and statistical analysis. Our findings suggest the neuroprotective effects of Montelukast on MAP-2-positive neuronal dendrites, presynaptic synaptophysin-positive terminals, and Iba-1-positive microglia in the cortex. Iba-1 also demonstrated a significant decrease of microglia in the hippocampus, an indication of neuroprotection in the brain. However, no other significant changes indicating neuroprotection were observed in HIV-gp120 transgenic mice treated with Montelukast.

Table of Contents

List of Figures:

CHAPTER 1- Investigating Neuroprotective Effects of Montelukast in HIVgp120 Transgenic Mice

Maxine Ortega[1], Marcus Kaul[1]

[1]Department of Biomedical Sciences, School of Medicine, University of California, Riverside, Riverside, CA, USA

Introduction

At the start of the epidemic, HIV treatment seemed unattainable with its rapid reproduction and death rates. Since the introduction of antiretroviral therapy (ART), HIV is a chronic yet manageable disease that has extended life expectancy significantly in those living with HIV. The first FDA-approved antiretroviral (ARV) drug was first introduced in 1987 as a mono-therapy treatment for those infected with HIV. In the mid-1990s, the development of new antiretroviral therapies arose and created various classes of ART based on their molecular mechanisms, such as nucleoside-analog reverse transcriptase inhibitors (NRTIs), non-nucleoside reverse transcriptase inhibitors (NNRTIs), integrase inhibitors, protease inhibitors (PIs), fusion inhibitors, and coreceptor antagonist (Arts & Hazuda, 2012). With the addition of new classes, the combination of different antiretroviral drugs to target more than one component of the viral life cycle became a common practice used to treat HIV-infected individuals. The combination antiretroviral therapy (cART) has played a huge role in significantly decreasing the number of HIV-related deaths and increasing the life expectancy of those who suffer from the virus. At the end of 2022, approximately 30 million people infected with HIV had access to ART, increasing by approximately 25% since 2010 (UNAIDS, 2022). Those suffering from the disease can now look forward to a longer life expectancy.

With its life-altering effects, ART does exhibit limitations in its overall protection of HIV and HIV-related complications. These limitations became pronounced when HIV-infected individuals still manifested neurocognitive impairments while being treated with cART (Kakad & Kshirsagar, 2020; Sacktor et al., 2002; Saylor et al., 2016; Yuan &

Kaul, 2021). As these neurological deficiencies due to the virus continued even with cART the term HIV-associated neurocognitive disorders (HAND) was introduced to describe all the different manifestations of neurocognitive dysfunction in patients. HAND is categorized based on severity into three different categories: asymptomatic neurocognitive impairment (ANI), minor neurocognitive disorder (MND), and HIV-associated dementia (HAD). Before cART, HAND prevalence was at approximately 50% of HIV patients, with an all-time high estimated to be 10-15% prevalence of HAD. The introduction of cART decreased the HAD prevalence by 75%, however, the ANI and MND had the opposite effect and increased its incidence in patients receiving cART (McArthur et al., 2010; Saylor et al., 2016). There was no overall change in the prevalence of HAND in the post-cART era suggesting the limitations of ART for neuroprotection.

Although ART suppresses the reproduction of HIV and reduces its viral load, findings suggest that the CNS harbors the virus in macrophages and microglia and uses them as mediators for neuronal damage seen in HAND patients (Kaul, Garden, & Lipton, 2001; Saylor et al., 2016). The current model of HIV neuropathology (neuro-HIV) demonstrates the binding of the HIV envelope protein, gp120, to CD4 and its one chemokine coreceptor, CXCR4 or CCR5, to activate or infect macrophages and microglia. As a result of this activation, various neurotoxic substances are released and contribute to neuronal damage and apoptosis. Some of these neurotoxic substances include excitatory amino acids, arachidonic acid, cytokines, chemokines, endothelial adhesion molecules, and free radical nitrate oxide through astrocytosis (Kaul, Garden, &

Lipton, 2001) The pathogenesis of HIV-neurodegeneration remains to be fully understood in its latter effects, making treatment options extremely difficult. Currently, no treatments exhibit complete neuroprotection from HIV, even with the beneficial effect of antiretroviral therapy on the life expectancy of HIV patients.

Previous work has targeted various key components involved in neuro-HIV to find ways to provide neuroprotection and restore behavioral functions. Arachidonic acid is one of the neurotoxic substances released by the activation of macrophages and microglia in neuro-HIV and its cascade events can potentially contribute to the upregulated inflammatory response that leads to neuronal damage (Kaul, Garden, & Lipton, 2001; Wang et al., 2021; Yuan et al., 2022). Arachidonic acid (AA) is a key substrate in the biosynthesis of eicosanoids, which contribute to inflammatory responses, immunoregulation, and involvement in the vascular, renal, gastrointestinal, and reproductive pathways. AA is metabolized to produce eicosanoids using three different pathways: COX pathways to form prostaglandins and thromboxanes, in the presence of cyclooxygenase, LOX pathways to form leukotrienes and lipoxins in the presence of lipoxygenase, and cytoP450 pathways to form hydroxyeicosatetraenoic acids (HETEs) and epoxyeicosatrienoic acids (EETs) in the presence of cytochrome P450 epoxyhydrolase. The effect of AAs in eicosanoid production is described as the arachidonic acid cascade. Eicosanoids, specifically the COX and LOX pathways, have evolved in inflammatory disease research as potential proinflammatory markers and are targets for treatment (Calder, 2020; Wang et al., 2021; Yuan et al., 2022).

Eicosanoids are currently being investigated for significant involvement in neuro-HIV and HAND, in anticipation of using them as potential therapeutic targets. The prevalence of eicosanoids has been shown in gene expression and cell quantification of both HIV animal models and infected cells, specifically leukotriene C4 synthase (LTC4S), the 5-LOX enzyme, and cysteinyl leukotriene receptor-1 (CysLTR1) (Albright & González-Scarano, 2004; Yuan et al., 2022). 5-LOX is the enzyme responsible for the initiation of the 5-LOX pathway and leads to the production of cysteinyl leukotrienes (LTC4, LTD4, LTE4) through the enzyme, LTC4S (Calder, 2020; Yuan et al., 2022). The exact role of eicosanoids in neuro-HIV remains to be completely understood, however, these findings provide momentum in this particular area of research and its potential neuroprotective properties for neuro-HIV treatment options.

Montelukast (MTLK) is an FDA-approved cysteinyl leukotriene receptor-1 antagonist drug that is used to inhibit the inflammatory response induced in asthma. In recent years, Montelukast has been investigated for other inflammatory diseases, such as coronary artery disease, type 2 diabetes mellitus, endocrine system diseases, and obesity, to see if it would have similar anti-inflammatory effects in these diseases (Wang et al., 2021). Montelukast has also been looked at as a potential neuroprotective agent for different neuroinflammatory diseases such as Alzheimer's and Parkinson’s Disease (Marschallinger et al., 2020; Nagarajan & Marathe, 2018). In these studies, they found a significant decrease in neuroinflammatory markers, alpha-synuclein and tumor necrosis factor-α, in transgenic and wild-type mice, which indicates the anti-inflammatory effect of MTLK that would potentially protect the brain from neuronal injury (Marschallinger et

al., 2020; Nagarajan & Marathe, 2018). With the new evidence of eicosanoids, MTLK is a new potential therapeutic agent that can be investigated for neuroprotection effects in HIV neuropathology.

This prospect of treatment in MTLK opens more doors to understanding the roles of eicosanoids in neuro-HIV and targets as potential therapeutic targets. Although ART has been the designated treatment for HIV, there are no current treatments or drugs for neuro-HIV. Without treatment options, HAND continues to pose a threat to the quality of life of people living with HIV, emphasizing the importance of the need for treatment. In this study, we will investigate the potential neuroprotective effects of Montelukast on HIVgp120 (gp120) and CCR5 WT mice. The administration of the treatments will be given over the course of 2 months, via voluntary oral administration or involuntary intraperitoneal injections. The treatments will be distributed in four groups: wild-type (WT) Saline, WT MTLK, HIVgp120 Saline, and HIVgp120 MTLK. Following the treatment, the animals will be euthanized and brain tissue harvested for histopathological evaluation using immunofluorescence staining and its quantitative analysis of neuro-HIV markers in the cortex (layer 3) and hippocampus (stratum radiatum). Given the published data, we expect to see decreased trends of activated microglia and reactive astrocytes as well as increased trends of dendrites and synapses in both treatments of WT animals and MTLK-treated gp120 mice, whereas the saline gp120 mice see the opposite trends that are associated with neuro-HIV.

Materials and Methods

Animal Model and Cohort

HIVgp120 (gp120) transgenic model is used as our animal model in this experiment because it manifests similar characteristics of human neuro-HIV. Neuro-HIV demonstrates a phenotype that can be observed by loss of neuronal dendrites and synapses, increased activation of microglia/macrophages and reactive astrocytes, and behavioral impairments (Maung et al., 2014; Thaney et al., 2018; Toggas et al., 1994). HIVgp120 mice express the soluble HIV envelope protein, gp120, of the HIV-1 LAV isolate in the brain (Maung et al., 2014; Toggas et al., 1994; Valentin et al., 2000). The envelope protein of HIV, gp120, is expressed on astrocytes and its encoding gene is regulated by the glial fibrillary acidic protein (GFAP) gene to create soluble forms of gp120 in mice (Toggas et al., 1994). Our GFAP-gp120 transgenic line can detect gp120 levels more easily, also called High Protein Express (HPX). The HIV-1 LAV isolate preferentially interacts with CXCR4, and infects primary macrophages (Valentin et al., 2000). The expressed, soluble gp120 of the HIV-1 LAV isolate triggers in the transgenic mice the characteristic neuro-HIV phenotype, including activation of microglia, and therefore can be considered the best-fit model for this experiment.

Our cohort of 32 male animals consisted of HIV-gp120 transgenic and non-transgenic, wild-type mice at the age of 12 months. Our WT and HIV-gp120 transgenic mouse model was originally provided by Dr. Lennart Mucke of the Gladstone Institute of Neurological Disease, University of California, Francisco, CA, USA. The mice have a mixed genetic background of SJL and C57BL/6 mouse strains. Other phenotype characteristics of the mice include a mixture of black and agouti mice (17 black and 15 agouti) and hair loss due to barbering, which suggests implications for social hierarchy in

same-sex cages (Kalueff et al., 2006). Out of the 32 mice, 18 were WT mice and 14 were gp120-transgenic (tg) mice, and the group of each genotype was split in half for saline and MTLK treatment. All animals were weighed throughout the experiment and no significant weight changes occurred in the mice, except one mouse, HPX 766, which lost 13% of its body weight (approximately 7 grams) from the beginning to the end of the experiment.

Montelukast treatment in HIVgp120 mice: Voluntary Oral Administration

Montelukast is administered to people as an oral medication for asthma treatment due to its quick absorption (Wermuth, Badri, & Takov., 2023). Studies have shown that Montelukast demonstrates some neuroprotective effects in neuroinflammatory disease through oral and injection administration to animal models. These studies have shown the efficacy of Montelukast in both 10-day and 42-day treatment administration (Marschallinger et al., 2020; Marschallinger et al., 2015; Nagarajan & Marathe, 2018). Oral administration for mice is done by intragastric oral gavage, which can potentially lead to stress that could be considered a confounding factor. In a study on cannabinoid-1 (CB1) receptor and neuropeptide Y interactions in the regulation of energy homeostasis, they used treatment administration through jellies and proposed a protocol for voluntary oral administration (Zhang, 2021; Zhang et al., 2010). Since MTLK is an oral treatment, we chose to use voluntary oral administration over an eight-week period, excluding weekends, to best fit the translation of MTLK treatment in our gp120 mouse model.

The voluntary oral administration protocol outlines the production of the treatment jellies and training for jelly intake by the mice (Zhang, 2021). The jelly production requires Royal (Royal Dessert, Eberbach, Germany) reduced calorie sugar-free gelatin and the powder form of the vehicle drug. We used strawberry, lime, orange, and cherry flavors to make the jellies more desirable to eat. Animals receiving MTLK were given a 10mg/kg dose per the average weight of the animal, 30 g. In previous studies, Montelukast was administered at 5 mg/kg and 10 mg/kg to animals with associated neuroinflammatory disease (Marschallinger et al., 2020; Marschallinger et al., 2015; Nagarajan & Marathe, 2018). In the Parkinson's study, the data showed a significant reduction of tumor necrosis factor-alpha in groups with MTLK 10mg/kg dose compared to the 5 mg/kg dose group (Nagarajan & Marathe, 2018). 40 g of jelly powder was measured out of the package and added to 10 mL of sterile boiled water. Montelukast sodium powder (Thermo Scientific, Waltham, MA, USA) was diluted into the jelly stock to obtain 3.2 mg/mL and 100 uL of stock was aliquoted into VWR Tissue Culture Plate 96 Wells-F, Surface Treated, Sterile (Avantor Science, Radnor, PA, USA). The plates were left in a 4-degree Celsius room overnight to solidify. The control animals received the same jelly but in stock with water.

In order to ensure voluntary feeding, the mice had to undergo jelly-dose training that has been outlined in the protocol for 'Voluntary oral administration of drugs in mice' (Zhang, 2021). According to the protocol, food was removed from each cage to fast animals overnight. Jellies were placed on a Nunclon Delta Surface (Thermo Scientific, Waltham, MA) and into the cages of each animal. Animals were placed in a feeding cage,

one feeding cage per housing cage, without bedding to ensure there were no distractions in the feeding process. Once one animal completed their feeding, the next animal would be placed in the cage with a new plate with new jelly. Training was expected to take up to 4 days for all animals to eat.

Unfortunately, not all of the mice ate their jellies within the anticipated jelly period. After the four-day period, we decided to continue with the voluntary feeding protocol and introduce the MTLK jellies to the designated animals for 4 weeks, however, the jelly feeding administration continued to have difficulties with complete feeding intake by all animals. This issue posed an inefficient intake of MTLK treatment that would affect our results and findings for potential neuroprotective effects in HIVgp120 mice, and after consideration, we decided to switch our means of administration to involuntary intraperitoneal injections.

Montelukast treatment in gp120 mice: Involuntary intraperitoneal injections

Intraperitoneal injections ensure that all our animals receive their respective treatments and a uniform administration. This administration would still be over an eight-week period and the same dosage regimen as described above was used for the injections. Montelukast sodium was diluted in sterile water to make a concentrated Montelukast stock of 30mg/mL and stored at – 20 degrees Celsius storage in amber vials for light protection. The control stock consisted of 0.9% sodium chloride (NaCl) solution. Montelukast injections were based on the weight of each animal. For example, the average weight of mice is 30 g with a dose of 10mg/kg of MLTK, this would translate to

the injection being 10 uL MTLK stock and 90 uL saline stock for a total volume of 100 uL per injection. For the first week, each animal was weighed prior to injections and then every Monday for the following seven weeks. They were weighed using Denver External Calibration (Denver Instruments, Arvada, Colorado, USA) and its multiple weighting units function for better accuracy. Mice were placed in a plastic cylinder tall enough to ensure mice did not try to jump out of the container and tared at zero grams to get the most accurate weight of the animals. Weights were recorded for the correct dosing of MTLK per animal as well as to observe any adverse reactions to the treatment. U 100 0.5 mL Insulin Syringes with the BD Micro-Fine IV needle (Becton Dickson, Franklin Lakes, NJ, USA) were used to inject solutions of the drug and vehicle. The intraperitoneal injection target site is the alternated lower right or left quadrant of the abdomen each day and injected at a 45-degree angle perpendicular to the abdomen to prevent puncture of any organs. Intraperitoneal injections are chosen to administer large volumes of injected substances consistently and quickly absorbed in the body. The only issue that occurred during the injections was the bubbling of the injected substance in mice, but this issue was resolved by administering another injection on the opposing side of the initial injection. No significant issues with intake occurred in the animals during the period of treatment that would be influence the data and results that we collected. Below in Figure 1 is an experimental timeline of the Montelukast treatment to animals and the switch over from voluntary feeding to involuntary injections.

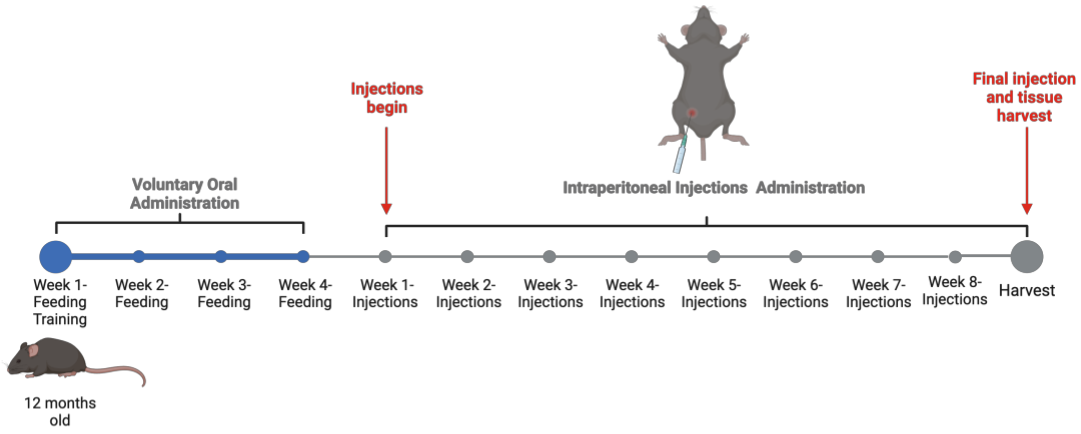

Figure 1. Timeline for Montelukast treatment. At the age of 12 months, mice began feeding training of jellies and continued our efforts of voluntary oral administration for four weeks. One we switched over, we administered Montelukast and saline solution intraperitoneal (IP) injection for 40 days (8 weeks). After the week 8, mice were injected the following Monday and tissue harvested their brain the same day.

Harvesting and Brain Slicing

Animals received their last injection the morning of their euthanization and brain tissue harvest. The brains were collected following terminal isoflurane anesthesia and exsanguination with cardiac perfusion with 0.9% saline solution. Tail biopsies were also taken for further analysis. In the animals selected for immunofluorescence staining, we collected one brain hemisphere and placed it in 4% PFA, 40 g of granulated PFA (Electron Microscopy Sciences, Hatfield, PA, USA) dissolve in 1 L PBS, dissolved by 1x PBS for the while other animal brains and immunofluorescence staining selected brain hemisphere were snap-frozen by liquid nitrogen to store for future assessments on brain tissue. Brains for immunofluorescence staining were sliced into 40-um sagittal sections using the Leica VT 1000S Vibrating blade microtome. Brains were sliced using a carbon steel injector blade at a speed of 5 and frequency of 9. We collected starting at slice 22 to make sure we got far enough into the medial brain. There was an error in slicing for two animals, HPX 738 and HPX 768. HPX 738 brain was sliced at 80 um making each slice twice as thick as the other, which cause some issues when mounting the brain upon the slide. I also caused z-stack of 40x air images to be an outlier for data analysis. Many of these images were unable to get data from because of the images' blurriness. HPX 768 was sliced at the same size, however, I caught the needed slice size of 40 um and disregarded of the thick slice samples. Unfortunately, the number of tissues collected from 85 to 32 slices collected from the animal. This issue did not affect the data extracted from the images.

Genotyping

Tail biopsies were collected in vials and used to confirm the genotype of each mouse. The lysis buffer used consisted of 332 uL of dH_2O, 40 uL of 1M Tris, 16 uL of 6 M NaCl, 8 uL of 10% SDS, 4 uL of 0.5M EDTA, and 2.5 uL of Proteinase K and was aliquoted at 400 uL to each vial then incubated overnight at 55 degrees Celsius. After the overnight incubation, 6 M NaCl was aliquoted into each tube at 250 uL and mixed. All vials were centrifuged for 10 minutes at maximum speed (16.1 rcf/13.2) at 4 degrees Celsius. 400 uL of the supernatant (no tail debris) was removed into a clean tube with the addition of 400 uL isopropanol and mixed until the formation of precipitate. Vials were centrifuged for another 10 mins, maximum speed at 4 degrees Celsius and isopropanol was removed from vials following centrifuge. Empty vials were placed in the Eppendorf Thermomixer R Mixer (Eppendorf, Hamburg, Germany) shaker at a speed of 1400 rpm for 30 mins. 70 % ethanol was added in aliquots of 500 uL to vials to sit for 5 minutes before centrifuging with Centrifuge 5430/5430 R- High- Speed Centrifuge (Eppendorf, Hamburg, Germany) at max speed (16.1 rcf/13.2) at room temperature. Ethanol was removed and vials were placed in a heat block at 55 degree Celsius for 45 minutes. TE buffer (500 uL of 1M Tris pH 8.5, 100uL 0.5 < EDTA, and 50 mL of H_2O) was added to each tube with 60 uL and flicked to make sure DNA made it into the solution, then left overnight at room temperature. Master mix for gp120 compromised of 8 uL of dH_2O, 0.5 uL of each primer, (203)gp120,1 (25 uM) 5’ – TCA GCC AAT TCC CAT ACA TTA

TTG and (204)gp120, 2 (25 uM) 5' CCT GTT CCA TTG AAC GTC TTA TTA TTA C, and 15 uL of GOTaq and 0.5 uL was added into DNA.

Once DNA was extracted from tail biopsies and the PCR reaction completed, the samples were analyzed through electrophoresis. Agarose gel must be formed through the mixture of 1x TBE, 2 grams of agarose, and 5.0 uL GelRed with a comb to form 20 wells. The gel was placed in the electrophoresis system and TBE was poured over to cover the gel. DNA marker (10 uL H_2O, 3 uL OG, and 1 uL DNA ladder) is added to each row of wells as well as 3 uL of OG. Each sample was added to each column at 13 uL. Electrophoresis is run at 167 volts for 35 minutes. After the electrophoresis is finished, agarose gel was analyzed using the imager- program to determine the genotype of all animals as shown in Figure 2.

Immunofluorescence Staining Vibratome Mouse Brain Slices and Deconvolution Microscopy

We used two different antibody combinations for immunofluorescence staining, anti- MAP2 + anti-GFAP and anti-Synaptophysin (SYP) + anti-Iba-1. Both protocols use the same steps, however, the difference is the primary antibodies used for the experiments. Each animal needed 5 slices for staining: one for both control (CTL) and IgG antibodies and three for target-specific antibodies. Slices for the cell marker staining were of the same slice number for each brain, ensuring the same spacing medial to lateral each ~440 μm apart from the other. All animals collected around 85 to 96 tissue slices, beginning the slice 1 is collected in the inner brain and moving toward the outer brain.

Control staining slices were collected at slice 24 MAP2-GFAP and 27 in SYP-Iba-1. IgG staining slices were collected at 25 in MAP2-GFAP and 28 in SYP-Iba-1. The antibody-specific staining slices were collected at slices 55, 67, and 79 in MAP2-GFAP and 56, 68, and 80 in SYP-Iba-1. All slices were washed with PBS three times in 5-minute increments and then permeabilized with 1% Triton X-100 in PBS for 30 minutes. After another three 5-minute washes in PBS, nonspecific binding sites were blocked in 10% heat-activated goat serum diluted in PBS containing 0.05% Tween 20 (PBS-T) for 90 minutes. After 90 minutes, the primary antibody mixtures were aliquoted to the relative wells and left overnight. Primary antibodies used in both experiments were 5% goat serum in PBS for the CTLs and IgG1 Kapp Mouse myeloma MOPC21 (Sigma) antibody diluted (1:200) in PBS for IgG. In the MAP2-GFAP staining, we used a 1:250 ratio of polyclonal rabbit anti-GFAP (DAKO) antibody and a 1:200 ratio of mouse monoclonal a-MAP2 clone HM2 (Sigma) antibody diluted in PBS. GFAP antibody is an astrocyte marker that indicates astrocytosis and its promoter is used to regulate gp120 gene expression. MAP-2 antibody is a neuronal dendrite marker for post-synaptic terminals, which exhibits damage in neuro-HIV brains. In the SYP-Iba-1 staining, we used a 1:125 ratio of rabbit polyclonal anti-Iba (WAKO) antibody and a 1:50 ratio of mouse monoclonal anti-synaptophysin (Sigma) antibody. Iba-1 antibody is a microglia marker, which can indicate the presence of neuro-HIV with its specific fluorescence signal is elevated. Synaptophysin is a presynaptic terminal marker and can also indicate neuro-HIV associated injury, if its presence is diminished. The next day, the slices did three 5-minute washes in PBS-T then all slices were concentrated in the secondary antibody

solution for 60 minutes, note that the wells had to be protected from light after the secondary antibody was aliquoted. The secondary antibodies solution contained a ratio of 1:200 Alexa Fluor 488 goat anti-rabbit (Invitrogen, Waltham, MA, USA), shown by green fluorescence, and 1:50 Rhodamine Red goat anti-mouse (Jackson ImmunoResearch, West Grove, PA, USA), indicated by red fluorescence, that were diluted in 5% goat serum. The secondary antibody solution was the same in both experiments. After 60 minutes, the slices did three 5-minute washes in PBS-T, still covered from light. Lastly, we stained for nuclear DNA with Hoechst solution for 5 minutes proceeding three 5-minute washes with PBS. All staining was done at room temperature. After the staining, slices were mounted on glass slides covered with 10 uL of Vectashield Mounting medium and electron microscopy covers slides (Electron Microscopy Sciences, Hatfield, PA, USA) and sealed with nail polish. The brain slices were stored in a -20-degree Celsius freezer until analysis by microscopy.

Images of cortex and hippocampus were captured for assessment of neuronal injury and astrocytosis analysis using a computer-aided Zeiss inverted Axiovert 100 M fluorescence microscope (Zeiss, Jena, Germany) with electronically controlled 3D stage and appropriate filler settings and Slidebook software (Intelligent Imaging Innovations (3i), Denver, CO, USA). Neuronal DNA is indicated by DAPI; MAP2 and SYP are indicated by CY3; and GFAP and Iba-1 are indicated by CY3. For MAP2-IBA, we captured images at 10x magnification of uniform settings in each region and staining. The cortex was captured with a field of 1280 x 1280 um and intensities of 40 ms for DAPI, 30 ms for FITC, and 400 ms for CY3. For the control and IgG-stained brains, only one

image was needed for analysis. For the specific antibody stains, five images were taken throughout the cortex. Layer 3 of the cortex was masked in the Slidebook software package to quantify area and intensities for data analysis. The hippocampus was captured with a wide field of 2048 x 2048 um and intensities of 40 ms for DAPI, 85 ms for FITC, and 550 for CY3. Only one image of the hippocampus was required for all brains. For SYP, we captured images at 40x magnification with uniform settings for each region. Both the cortex and hippocampus were captured with a wide field of 688 x 688 um. Intensities for the cortex include 100 ms for DAPI and 1300 ms for CY3 and for the hippocampus z for DAPI and y for CY3. Five images of both regions were taken with image stacks at 0.5-um steps along the z-axis for each brain. Iba-1 images were captured with 10x magnification under uniform regional settings. Cortical images were captured at a 1280 x 1280 wide field with intensities of 50 ms for DAPI and 400 ms for Iba-1. Hippocampal images were captured at 2048 x 2048 um with intensities of 40 ms and 350 ms. Similar to MAP2-GFAP stains, we captured 5 cortical images and 1 hippocampal image. To analyze the 10x magnification, we masked each region for quantification of area and fluorescence intensities that we exported from the Slidebook software package. To analyze for SYP, images must be deconvolved with a constrained iterative algorithm and masked accordingly for fluorescence and volumetric quantification. Examples of masks for each staining can be found below in Figure 2.

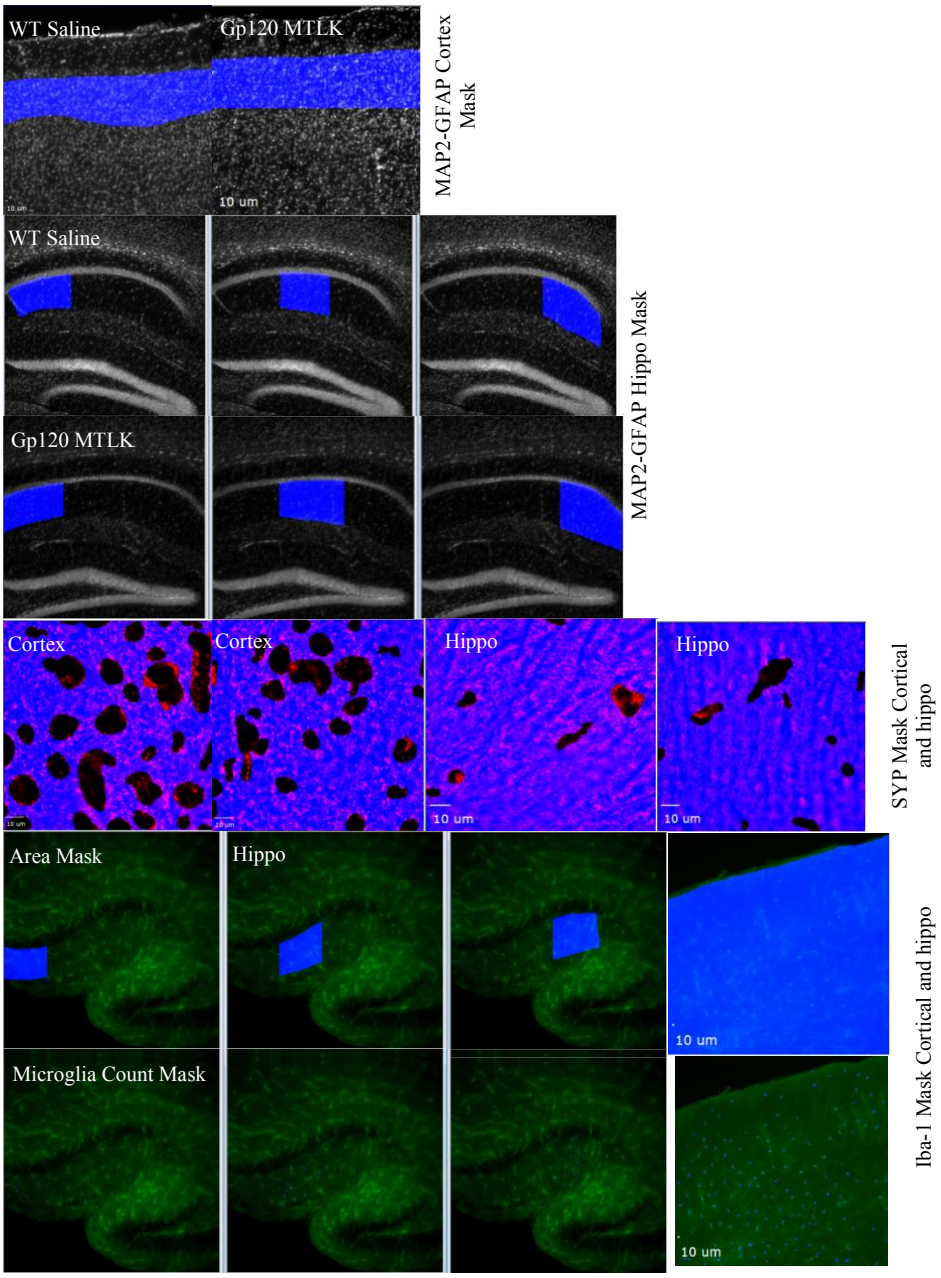

Figure 2. Cortical and hippocampal images and their respective masks for different staining. All masks are represented by the blue sections of the images. Immunofluorescence staining for MAP2/GFAP in the cortex enables the quantification of astrocytes and neuronal dendrites in cortex layer 3 (L3), which is shown by the mask drawn in the image. The mask for the hippocampus is divided into three equally drawn sections for one brain. Synaptophysin (SYP) is seen in the neuropil area of the cortex and hippocampus. Neuropil is a refined mask created by subtracting the cell bodies from the mask of the total image area minus blurry sections. The area of SYP+ neuropil is determined using a mask generated by threshold segmentation for the area. Iba-1 is masked by microglia count and total area of the cortex and hippocampus. Hippocampus is segmented into three fields to calculate more accurate count/mm2.

Results

PCR confirmation in DNA Genotyping of gp120 animals

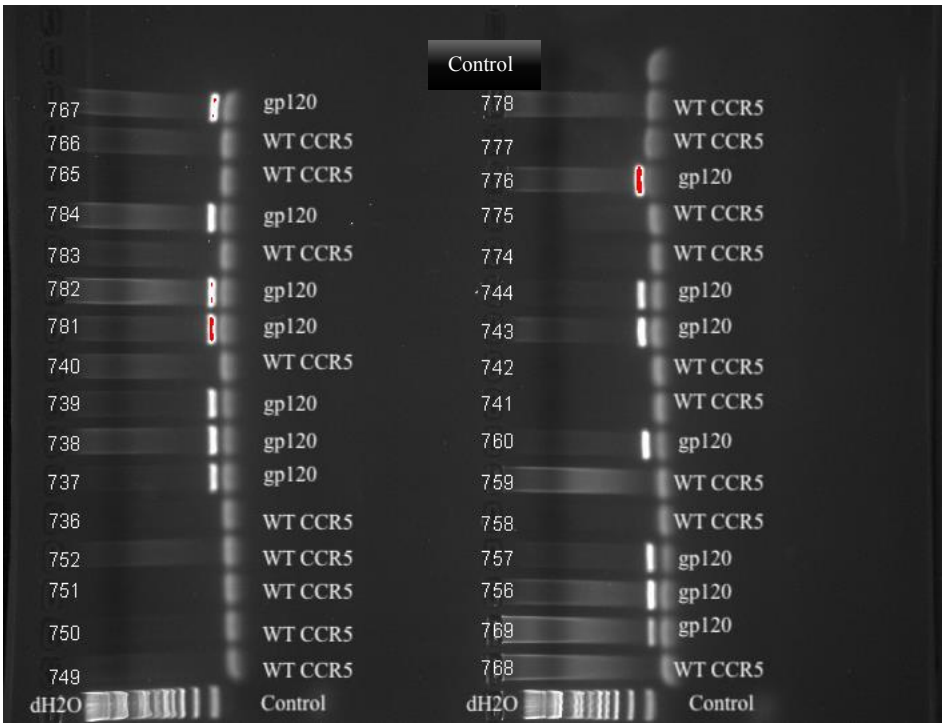

Figure 3. PCR Amplification for Genotype Confirmation of HIVgp120 Transgenic and Non-transgenic Control Mice. Visualization of gp120-specific band. PCR product using agarose gel electrophoresis (1.3% agarose). dH_2O is used as control whereas the control column demonstrates the supernatant mixture with primers to run through the electrophoresis as another indication the gel electrophoresis was conducted efficiently. Genes of gp120 mice are indicated by the red fluorescent band.

Statistical Analysis

Raw data of fluorescence exposure and its area or volume characterizing the various masks (shown in Figure 2) were exported from Slidebook software using the refine mask tool to export mask area and fluorescent intensity. The data was then compiled in Microsoft Excel. Statistical analysis was performed using the software GraphPad Prism version 8 (GraphPad Software, San Diego, CA, USA). Multigroup comparison was analyzed using One-Way ANOVA followed by Fischer's LSD post hoc test to not correct for multiple comparisons, whereas Turkey compares across multiple groups. We used this particular post hoc test to determine the standard error rate for each individual group, instead of comparing the error between multiple groups. This test is used for our experimental data can be compared and determine outliers within the group. The definition of statistical significance ranges from no significance to intense significance by p-values ($p > 0.05$ (ns), $p \leq 0.05$ (*), $p \leq 0.01$ (**), $p \leq 0.001$ (***), $p \leq 0.0001$)) with an N=3 animal per group; slices vary based on regional section and magnification.

Quantitative Analysis of Montelukast Treatment Effect on Neuro-HIV Markers Demonstrates Trends of Potential Neuroprotective Effects of MAP2 Markers in Neuro-HIV

The microtubule-associate protein-2 (MAP-2) is a biomarker for neuronal injury in neuro-HIV infection. Following the activation of microglia and macrophages, neurotoxic substances—including cytokines—are released. Through astrocytosis, these toxins contribute (directly and indirectly) to damage in the dendrites. Montelukast

treatment in gp120 mice demonstrates a significant increase in cortical MAP-2 ($p \leq 0.05$) in comparison to gp120 mice treated with saline (shown in Figure 4). This finding may suggest some neuroprotective effects of MTLK on neuronal dendrites in neuro-HIV brains. Although DAPI demonstrates a significant increase in all groups compared to WT saline mice, these results are inconclusive about the effect of MTLK on neuronal DNA in gp120-treated mice. WT mice should not have shown decreased neuronal DNA which flags alarm and suggests looking back at the data that was calculated. The increase of glial fibrillary acidic protein (GFAP), an astrocyte biomarker, indicates the incidence of astrocytosis, a phenotypic characteristic of gp120 mice, in both the cortex layer 3 and stratum radiatum shown in Figure 4. The gp120 gene sequence is also regulated by the GFAP promoter, so an increase in astrocytosis in gp120 mice is to be expected. Our results show this trend of increased GFAP in gp120 mice is consistent with the phenotype of neuro-HIV but MTLK does not show protection from astrocytosis. Our results suggest that MTLK protects neuronal dendrites and further research can investigate the efficiency of treatment and potentially the mechanism of MTLK inhibition in neuro-HIV.

In the hippocampus, there are similar trends of neuronal markers as seen in the cortex L3. Unfortunately, the data does not show significant differences between MTLK-treated gp120 mice compared to gp120 mice treated with saline. We quantified our data by normalizing the area of the mask through the division of our sum intensity by the area in microns and multiplying this ratio by 1×10^6, which is shown in Figure 5. Our data suggests some cortical neuroprotective effects of MAP-2 with MTLK treatment from increased incidence of neuronal dendrites, which is typically decreased in gp120

neuropathology (Shown in Figure 5). DAPI is shown to have decreased with the MLTK-treated WT mice and led to inconclusive results of MTLK effect on DAPI as this is not a phenotype of neuro-HIV. Our data in the cortex shines light on use of MTLK as a potential treatment for people living with HAND.

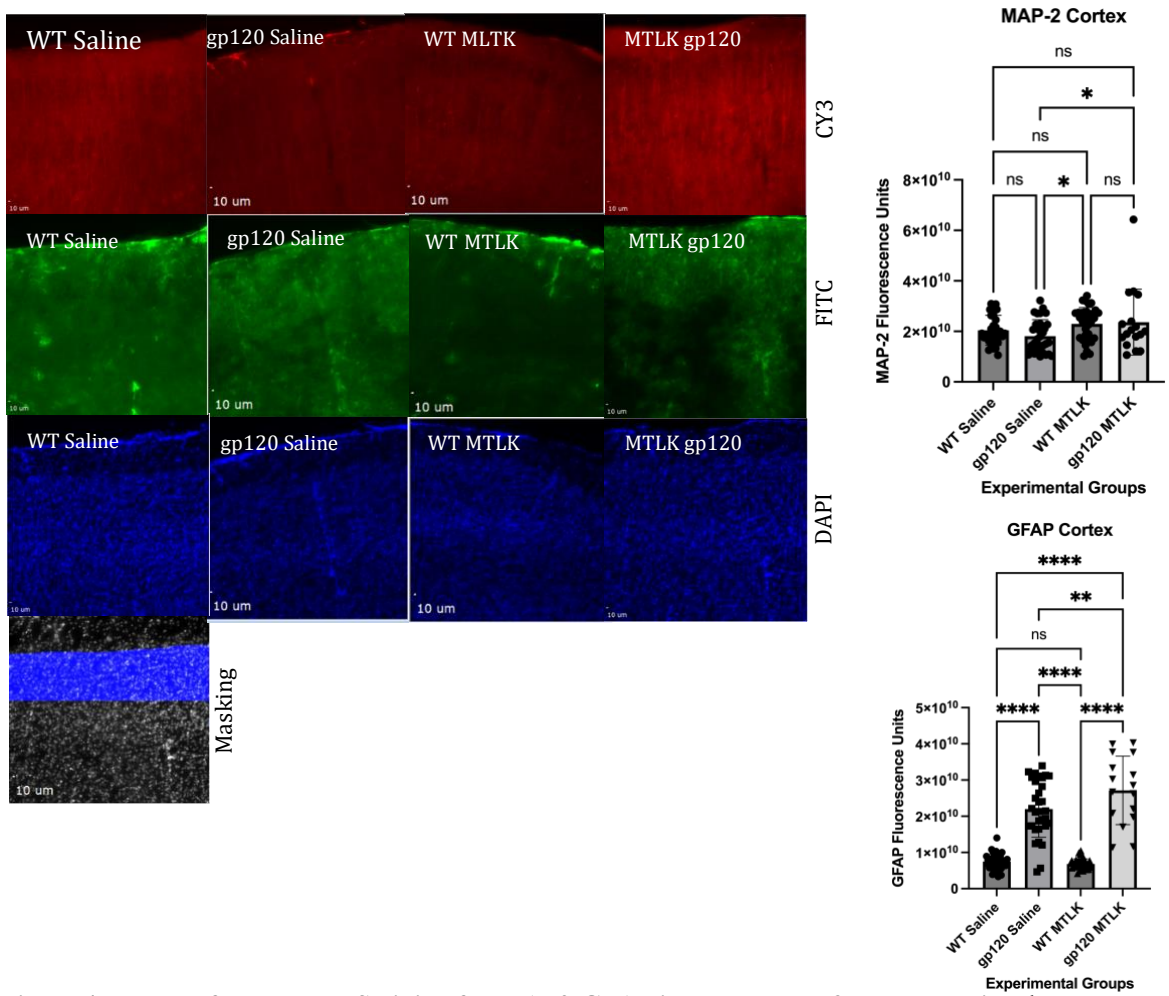

Figure 4. Immunofluorescence Staining for MAP2-GFAP in cortex layer 3 data analysis. The cortex and hippocampus are stained with Rhodamine Red indicated by the red fluorescent intensity, which is our secondary marker to quantitate MAP-2 in the brain for analysis. MAP-2 demonstrates a significant increase in MAP-2 quantity in the cortex, p-value is $p \leq 0.05$. MAP-2 also increases in the hippocampus, however, there is no statistical significance to validate these results. MTLK can be shown to have a neuroprotective effect in gp120 mice. Phenotypic trends seen in patients with HAND are demonstrated in our results for both the hippocampus and cortex such as increased astrocytosis, indicated with GFAP/FITC results. Whisker pot indicates the mean and range of the data set. N= 3, 5 slices per animal, 3 fields per specific antibody staining, and 1 per non-specific staining and control. The definition of statistical significance ranges from no significance to intense significance by p-values ($p > 0.05$ (ns), $p \leq 0.05$ (*), $p \leq 0.01$ (**), $p \leq 0.001$ (***), $p \leq 0.0001$))

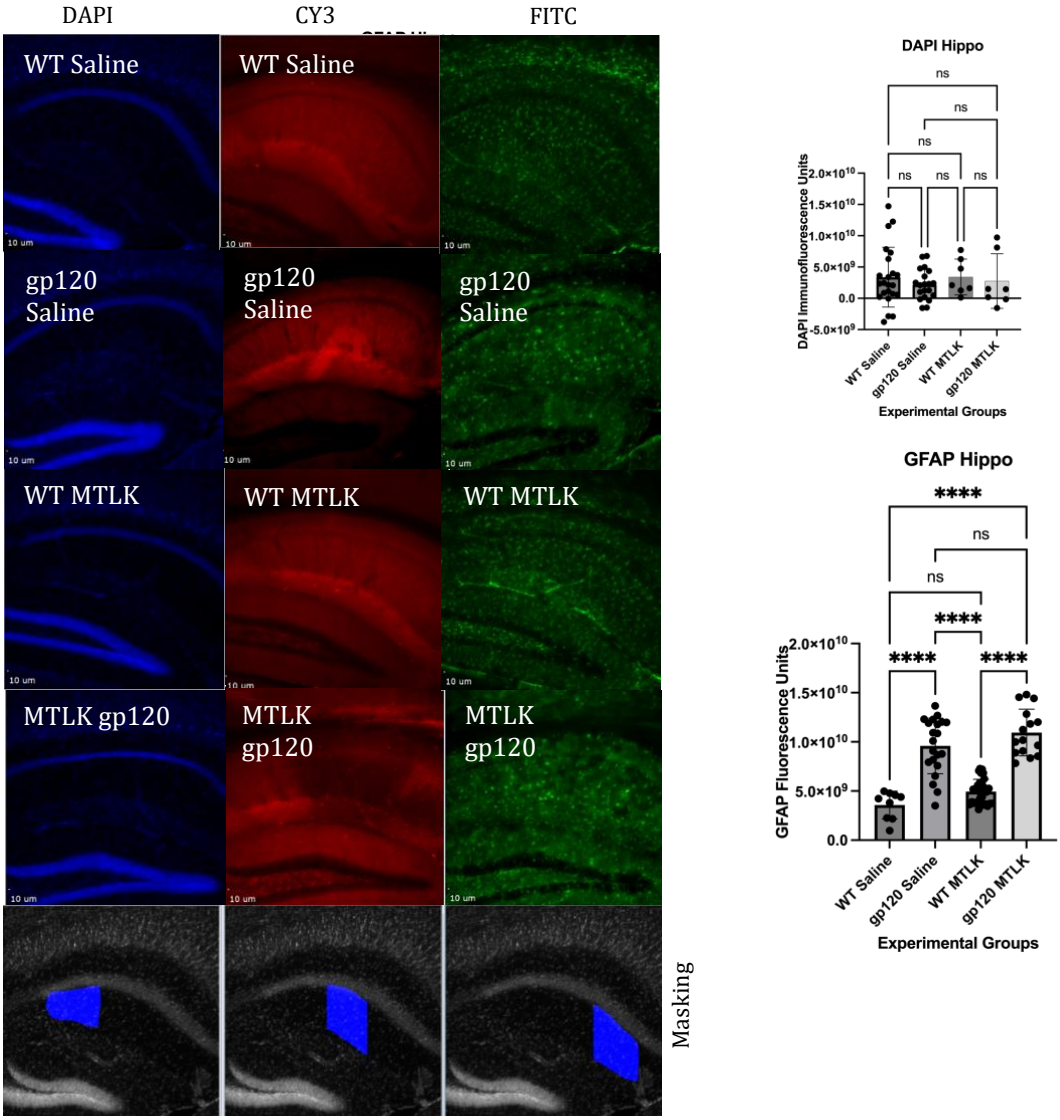

Figure 5. Immunofluorescence Staining for MAP2 and GFAP in the hippocampus stratum radiatum. There are no significant indications of neuroprotection of MTLK in gp120 treated mice. DAPI, blue fluorescence, data does not reflect the phenotypic characters of neuro-HIV. Neuronal DNA should be the lower in the gp120 saline as neuronal DNA because neurons are damaged and destroyed in HIV neuropathology. Increase of astrocytes, GFAP marker, is shown to affect gp120 groups. The definition of statistical significance ranges from no significance to intense significance by p-values ($p > 0.05$ (ns), $p \leq 0.05$ (*), $p \leq 0.01$ (**), $p \leq 0.001$ (***), $p \leq 0.0001$))

Quantitative Analysis of Synaptophysin and Iba-1 in Cortex and Hippocampus Demonstrates Need for Further Research of Montelukast Treatment in Neuro-HIV

Neuropil was calculated based on the red CY3 signal of synaptophysin without the hollow cell bodies that appear in the figure like black holes, which can be seen in Figure 6, for both hippocampal and cortical images. We use the mean and median of synaptophysin sum intensities to determine the cutoff for a new mask that exhibits the best intensity to capture all synaptophysin signals in the images. We extracted this mask without the cell bodies to quantify the data. We determine the cutoff by using the closest mean and median of volume multiplied by 1.025, 1.050, 1.075, and 1.1 for all groups (WT saline, WT gp120, WT MTLK, and MTLK gp120). The cutoff chosen for the data below was 1.025 for WT animals and gp120 MTLK mice then 1.075 for the gp120 Saline group as these intensity means and medians are similar to one another. We inserted a new mask for all images with their respective intensities and exported data to determine the percentage of synaptophysin in the neuropil. Synaptophysin + neuropil percentage is calculated by cut-off mask without cell bodies divided by the volume of neuropil multiplied by 100 for the percentage. Our data shown in Figure 6 shows significant effects that indicate an increase of the pre-synaptic terminals in gp120-treated mice compared to gp120 saline mice and potential neuroprotective effects of MTLK. The hippocampus results do not reflect characters of HIV neuropathology in the SYP+ Np%. WT and gp120 MTLK treated mice both showed a significant decrease of Np% than the saline treatment, which cannot conclude any suggestions from data as WT MTLK mice should not demonstrate a decrease in SYP+ Np%. Although these results are not favorable, we want to continue investigating the data collected in this staining to see if

there are any confounding variables contributing to the data shown. For this stain, N=3 animals, 5 slices per animal, 5 fields in the cortex and hippocampus. All SYP data and images are shown below in Figure 6.

Resident microglia in the brain can be indicated by the green FITC signal and is the biomarker for anti-Iba-1 antibodies in the hippocampal stratum radiatum and cortex. Microglia were manually counted and masked by individual dots to present each microglia all throughout the cortex and stratum radiatum. The total area masks the cortex and stratum radiatum of the hippocampus for calculating the microglia count/mm2. Results of the Iba-1 data analysis show a decrease in microglia count of MTLK-treated gp120 mice compared to gp120 saline mice. The phenotype of neuro-HIV demonstrates an increase of activated microglia in the cortex and hippocampus. Our results suggest MTLK inhibition of microglia activation in the cortex and hippocampus of gp120-treated mice from the decreased presence of microglia in this group. Data and images are shown below in Figure 7.

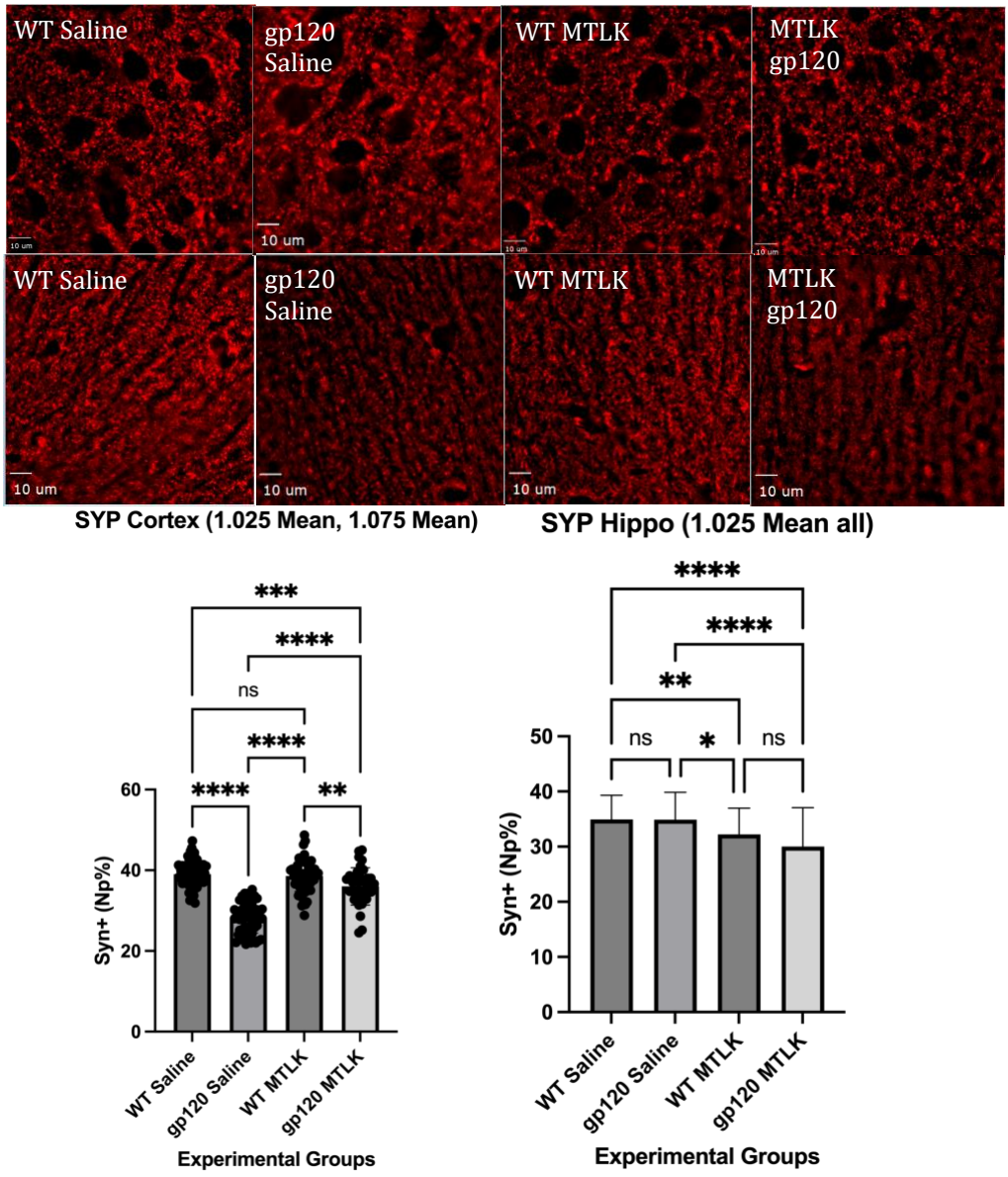

Figure 6. Immunofluorescence Staining for SYP in the cortex and hippocampus stratum radiatum. SYP results in the cortex demonstrate neuroprotective effects in gp120 MTLK mice. SYP marks pre-synaptic terminals in the cortex and hippocampus and increase signal of MTLK gp120 mice indicates intact terminal compared to gp120 Saline mice. There are no significant indications of hippocampal neuroprotection of MTLK in gp120 treated mice. N=3 per group, 5 slices per animal, and 5 fields for both cortex and hippo. The definition of statistical significance ranges from no significance to intense significance by p-values ($p > 0.05$ (ns), $p \leq 0.05$ (*), $p \leq 0.01$ (**), $p \leq 0.001$ (***), $p \leq 0.0001$))

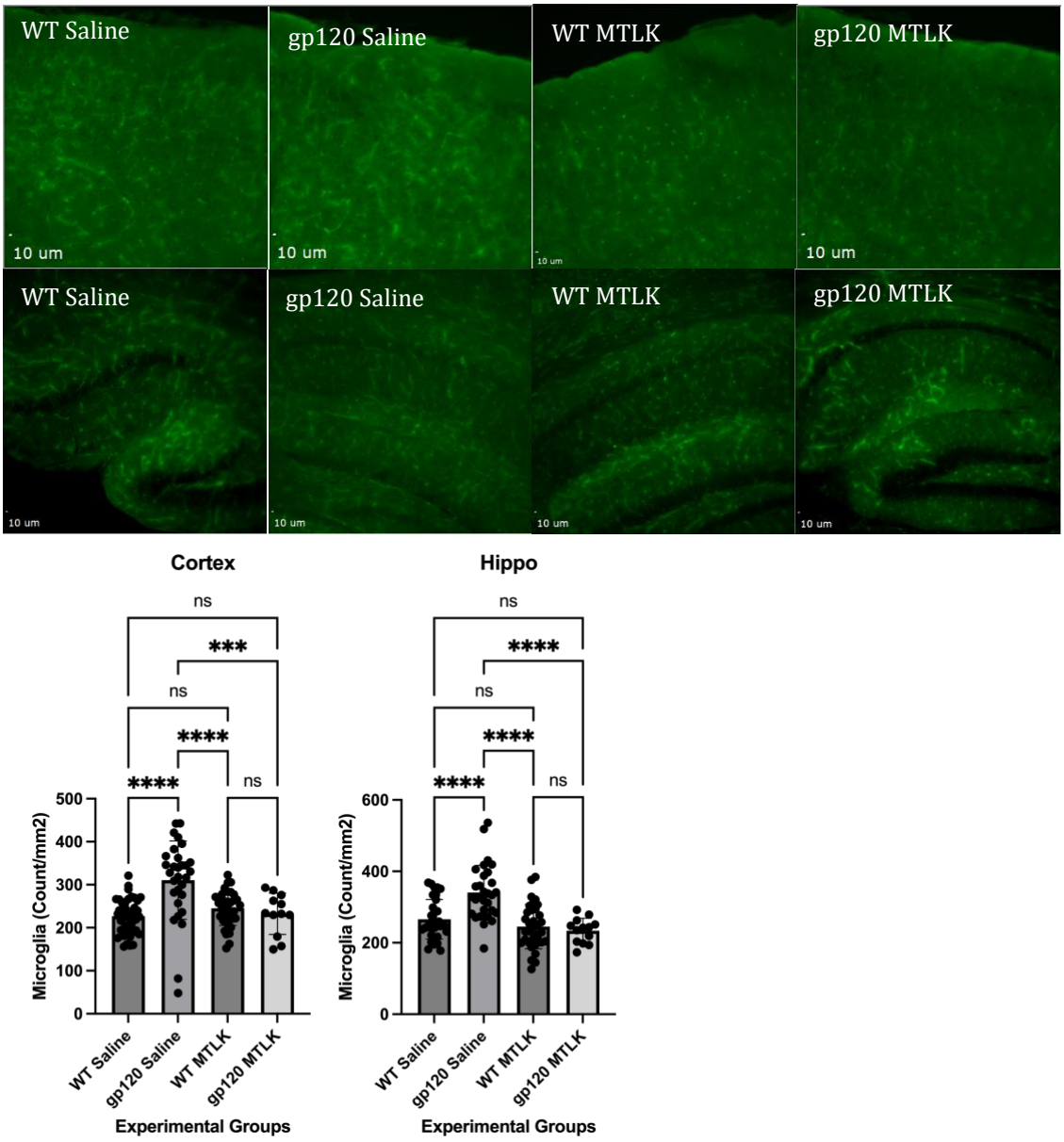

Figure 7. Immunofluorescence Staining for Iba-1 demonstrate significant decrease of microglia in the cortex and hippocampus stratum radiatum. Anti-Iba-1 antibody stains for biomarker, microglia, in the cortex and stratum radiatum, which increases in the presence of neuro-HIV. Our data shows a significant decrease of microglia in MTLK treated gp120 mice in both the cortex and stratum radiatum. These results suggest neuroprotection of microglia in the neuro-HIV affected regions in the brain, cortex and stratum radiatum. N= 3 animals per group, 5 brains per animal, and three fields in the cortex and one field in the hippocampus per animals. The definition of statistical significance ranges from no significance to intense significance by p-values ($p > 0.05$ (ns), $p \leq 0.05$ (*), $p \leq 0.01$ (**), $p \leq 0.001$ (***), $p \leq 0.0001$))

CHAPTER 2- Discussion

Maxine Ortega[1], Marcus Kaul[1]

[1]Department of Biomedical Sciences, School of Medicine, University of California, Riverside, Riverside, CA, USA

Summary

There is no current treatment for patients living with HAND, and since the introduction of ART, the percentage of people living with HAND has remained the same, but asymptomatic neurocognitive impairment (ANI) and minor neurocognitive disorder (MND) have increased its prevalence. These neurological complications can impair day-to-day activities and affect the overall quality of life experienced by infected individuals. With recent studies investigating the relationship between eicosanoids and neuro-HIV arising, new doors are opened for potential treatment in protection against HIV neuropathology. Montelukast has been studied for its potential protective effects in neuroinflammatory diseases such as Alzheimer's and Parkinson's Disease. The data from these studies support and suggest some neuroprotective power of MTLK due to its anti-inflammatory properties. These findings led us to investigate the effects of MTLK in HIVgp120 transgenic mouse models, which best present characteristic manifestations of neuro-HIV.

Our 8-week study initially used the protocol of voluntary feeding methods of the Montelukast treatment in jellies. After 4 weeks of voluntary oral administration, there were still issues with getting the entire cohort to eat their jellies. This issue may have occurred due to the age of the mice which can indicate a decrease in the appetite of the mice. The preliminary procedure for voluntary oral administration used 6-month-old mice and had success with their administration, which could indicate the aging effects on the eating habits of the mice. With inconsistent feeding behaviors, we decided to switch our method to involuntary injections. Each animal received 10 mg/kg of Montelukast

based on the animal's body weight and administered via intraperitoneal injections. Once the 8 weeks were over, we administered our last injection, and following the final injection, harvested their tissues brains to quantify the data and interpret the effect of MTLK for neuroprotection in HIV.

We quantified our data through Slidebook software by drawing masks over our regions of interest and cell counting to determine the number of cells and the determine the intensity quantification in our images. Through the statistical analysis of the data exported from Slidebook, we found a significant increase of MAP-2 in the immunofluorescent intensity comparison with control or IgG stained images and SYN+ Np% in the cortex of MTLK gp120 mice compared to the gp120 saline. Hippocampus did not find any significant protective effects in MAP-2 or SYN + Np%. Astrocytes in GFAP staining did not show any protection in MTLK but demonstrated an increase of astrocytes in both regions of interest, and interestingly, gp120 mice demonstrated upregulation of astrocytosis. Finally, Iba-1 staining results significantly decrease in microglia (count/mm3) of both the cortex and stratum radiatum, which show upregulation in gp120 saline mice and in neuro-HIV, therefore, indicates neuroprotection of microglia in MTLK treatment. These results suggest some neuroprotection of MTLK in gp120 mice compared to the saline-treated mice.

Conclusions

Montelukast has demonstrated some protective effects of neuro-HIV phenotypes such as an increase of SYN+ Np% and MAP-2 in comparison to control and IgG stains

and a decrease in activated cortical and hippocampal resident microglia. Montelukast should be investigated more as a potential neuroprotective agent in HIV neuropathology with more findings suggesting its protective effects in neuroinflammatory diseases. Our cortex data of MAP-2 and SYN + Np% can suggest inhibition of the inflammation that leads to injury in the neuronal dendrites, which typically has a decrease in the incidence of neuro-HIV presentations. Microglial anti-Iba-1 antibody expresses a decrease of microglia presence in the stratum radiatum and cortex of gp120 MTLK treated mice, which is seen as upregulated in neuro-HIV phenotypes.

Although there were significant results for neuroprotection in MTLK-treated gp120 mice, there were still issues that we ran into throughout the experiment. For instance, the voluntary oral administration could have had several problems that resulted in the poor outcome of predicted intake. The age of the mice, 12 months old, at the start of the experiment, was significantly older than the mice in the original protocol. At the age of 12 months, mice are closer to the end of their life as their life expectancy is 16 months for HPX mice. This difference in age can indicate a potential confounding variable in the appetite of the older mice and hence decrease the intake likeliness of these mice. The jellies did not have the exact composition of jellies indicated in the protocol by Zhang, 2021. Our jellies used in the experiment were premade sugar-free gelatin from Royal Desserts (Royal Dessert, Eberbach, Germany), which could have had an adverse taste on the mice upon intake. There was also a difference in the size of the jellies. The jelly size in the protocol was 237.5 uL compared to our jellies at 100uL, increasing in size by 102.3%. These differences could have contributed to the troubles in voluntary

oral feeding of the mouse cohort. Other issues we ran into during the experimental timeline occurred in the data analysis of some immunofluorescence stains. These issues are presented in our data with inconsistent gp120 phenotypic characteristics throughout our analysis. These inconsistencies manifested DAPI and MAP-2 stains and demonstrated an upregulation of both biomarkers in gp120 mice that should usually exhibit lower levels of these markers in neuro-HIV brains. Based off the images and data we used for these analyses suggest an inconsistent area of masking between the captured field images, ranging from 5×10^9 to 4.5×10^{10} sum intensity/normalized area, which can produce large data variations and inconsistencies dad leading to phenotypic characteristics of neuro-HIV brains.

Montelukast has demonstrated inhibition of cortical neuronal damage and microglia activation in treated HIVgp120 mice. With the support of these results, these findings should encourage more research into MTLK as a potential treatment for patients with HAND. Although there was only inhibition of activated microglia in the hippocampus, the data suggests some protection against neuro-HIV infection and can encourage further research to investigate protection in the hippocampus. The lack of protection in MTLK-treated gp120 mice represented through our data could have been due to the area masking inconsistencies for all stains except Iba-1. However, this data can be used to propel research in potential treatments for neuro-HIV in hopes of increasing neurocognition in HIV-infected individuals and decreasing the incidence of HAND in HIV patients.

Future Directions

Montelukast has been shown to provide some neuroprotective effects from neuronal damage through the increase of neuronal dendrites and decrease of activated microglia, opposing phenotypic characteristics in neuro-HIV. We could also perform other experiments that can be used to confirm these findings that our data suggests. For instance, we can use the qPCR genotyping of our tissue samples to confirm the increase of neuronal dendrites and pre-synaptic terminals and decrease microglia incidence by confirming their associated amino acids quantifications and exhibiting the same trends found in our preliminary data. Microglia count can proliferate in the brain with the introduction of foreign substances. Anti-Iba-1 antibody, a microglial marker, also indicates other monocytes present in the brain. In order to confirm the presence of microglia, we can also conduct a flow cytometry analysis to investigate the microglia structure in MTLK and saline-treated gp120 and WT tissue samples to compose the microglia's physical characteristics. We can then distinguish activated microglia from other monocytes as well as proliferated microglia to further support our findings.

With the benefits of voluntary oral administration, our lab has used this method of administration with MTLK in gp120 and WT animals, but at a much younger age, 6-month-old mice. Jelly intake of the entire cohort was seen and voluntary oral administration was successful in their experiment. This success indicates the potential effects of increasing age in our cohort could have been the contributing factor to our failure in this voluntary administration of MTLK jellies. Once MTLK is investigated more for neuro-HIV treatment, I would suggest doing a study with tissue from gp120

mice and the combination therapy of cART and MTLK to investigate any potential toxicity or efficiency of drugs administered together since HIV individuals have more access to cART and those exhibiting HAND must live long enough for this infection to develop, which suggests that most people who need this treatment are utilizing cART drug. One group of gp120 mice can be administrated cART and Montelukast and the other group can receive just Montelukast. We can do similar experiments to quantify the findings from our tissue collections.

These experiments can eventually lead to the potential use of MTLK in HAND patients and investigate neuroprotective effects that are manifested in human with HAND, which is the ultimate goal of Montelukast treatment in neuro-HIV.

References

Albright, A. V., & González-Scarano, F. (2004). Microarray analysis of activated mixed glial (microglia) and monocyte-derived macrophage gene expression. *J Neuroimmunol*, *157*(1-2), 27-38. https://doi.org/10.1016/j.jneuroim.2004.09.007

Arts, E. J., & Hazuda, D. J. (2012). HIV-1 antiretroviral drug therapy. *Cold Spring Harb Perspect Med*, *2*(4), a007161. https://doi.org/10.1101/cshperspect.a007161

Calder, Philip C. (2020). Eicosanoids. *Essays in Biochemistry*, *64*(3), 423-441. https://doi.org/10.1042/ebc20190083

Kakad, S. P., & Kshirsagar, S. J. (2020). Neuro-AIDS: current status and challenges to antiretroviral drug therapy (ART) for its treatment. *Current Drug Therapy*, *15*(5), 469-481.

Kalueff, A. V., Minasyan, A., Keisala, T., Shah, Z. H., & Tuohimaa, P. (2006). Hair barbering in mice: Implications for neurobehavioural research. *Behavioural Processes*, *71*(1), 8-15. https://doi.org/https://doi.org/10.1016/j.beproc.2005.09.004

Kaul, M., Garden, G. A., & Lipton, S. A. (2001). Pathways to neuronal injury and apoptosis in HIV-associated dementia. *Nature*, *410*(6831), 988-994. https://doi.org/10.1038/35073667

Marschallinger, J., Altendorfer, B., Rockenstein, E., Holztrattner, M., Garnweidner-Raith, J., Pillichshammer, N., Leister, I., Hutter-Paier, B., Strempfl, K., Unger, M. S., Chishty, M., Felder, T., Johnson, M., Attems, J., Masliah, E., & Aigner, L. (2020). The Leukotriene Receptor Antagonist Montelukast Reduces Alpha-Synuclein Load and Restores Memory in an Animal Model of Dementia with Lewy Bodies. *Neurotherapeutics*, *17*(3), 1061-1074. https://doi.org/10.1007/s13311-020-00836-3

Marschallinger, J., Schäffner, I., Klein, B., Gelfert, R., Rivera, F. J., Illes, S., Grassner, L., Janssen, M., Rotheneichner, P., Schmuckermair, C., Coras, R., Boccazzi, M., Chishty, M., Lagler, F. B., Renic, M., Bauer, H.-C., Singewald, N., Blümcke, I., Bogdahn, U., . . . Aigner, L. (2015). Structural and functional rejuvenation of the aged brain by an approved anti-asthmatic drug. *Nature Communications*, *6*(1), 8466. https://doi.org/10.1038/ncomms9466

Maung, R., Hoefer, M. M., Sanchez, A. B., Sejbuk, N. E., Medders, K. E., Desai, M. K., Catalan, I. C., Dowling, C. C., de Rozieres, C. M., Garden, G. A., Russo, R., Roberts, A. J., Williams, R., & Kaul, M. (2014). CCR5 Knockout Prevents Neuronal Injury and Behavioral Impairment Induced in a Transgenic Mouse

Model by a CXCR4-Using HIV-1 Glycoprotein 120. *The Journal of Immunology*, *193*(4), 1895-1910. https://doi.org/10.4049/jimmunol.1302915

McArthur, J. C., Steiner, J., Sacktor, N., & Nath, A. (2010). Human immunodeficiency virus-associated neurocognitive disorders: Mind the gap. *Ann Neurol*, *67*(6), 699-714. https://doi.org/10.1002/ana.22053

Nagarajan, V. B., & Marathe, P. A. (2018). Effect of montelukast in experimental model of Parkinson's disease. *Neurosci Lett*, *682*, 100-105. https://doi.org/10.1016/j.neulet.2018.05.052

Sacktor, N., McDermott, M. P., Marder, K., Schifitto, G., Selnes, O. A., McArthur, J. C., Stern, Y., Albert, S., Palumbo, D., Kieburtz, K., De Marcaida, J. A., Cohen, B., & Epstein, L. (2002). HIV-associated cognitive impairment before and after the advent of combination therapy. *Journal of NeuroVirology*, *8*, 136-142. https://doi.org/DOI: 10.1080/13550280290049615

Saylor, D., Dickens, A. M., Sacktor, N., Haughey, N., Slusher, B., Pletnikov, M., Mankowski, J. L., Brown, A., Volsky, D. J., & McArthur, J. C. (2016). HIV-associated neurocognitive disorder — pathogenesis and prospects for treatment. *Nature Reviews Neurology*, *12*(4), 234-248. https://doi.org/10.1038/nrneurol.2016.27

Thaney, V. E., Sanchez, A. B., Fields, J. A., Minassian, A., Young, J. W., Maung, R., & Kaul, M. (2018). Transgenic mice expressing HIV-1 envelope protein gp120 in the brain as an animal model in neuroAIDS research. *J Neurovirol*, *24*(2), 156-167. https://doi.org/10.1007/s13365-017-0584-2

Toggas, S. M., Masliah, E., Rockenstein, E. M., Rail, G. F., Abraham, C. R., & Mucke, L. (1994). Central nervous system damage produced by expression of the HIV-1 coat protein gpl20 in transgenic mice. *Nature*, *367*(6459), 188-193. https://doi.org/10.1038/367188a0

UNAIDS. (2022). *Global HIV & AIDS statistics — Fact sheet*.

Valentin, A., Trivedi, H., Lu, W., Kostrikis, L. G., & Pavlakis, G. N. (2000). CXCR4 mediates entry and productive infection of syncytia-inducing (X4) HIV-1 strains in primary macrophages. *Virology*, *269*(2), 294-304. https://doi.org/10.1006/viro.1999.0136

Wang, B., Wu, L., Chen, J., Dong, L., Chen, C., Wen, Z., Hu, J., Fleming, I., & Wang, D. W. (2021). Metabolism pathways of arachidonic acids: mechanisms and potential therapeutic targets. *Signal Transduction and Targeted Therapy*, *6*(1), 94. https://doi.org/10.1038/s41392-020-00443-w

Wermuth, H. R., Badri, T., & Takov., V. (2023, Updated 2023 Mar 22). *Montelukast*. Treasure Island (FL): StatPearls Publishing. https://www.ncbi.nlm.nih.gov/books/NBK459301/

Yuan, N. Y., & Kaul, M. (2021). Beneficial and Adverse Effects of cART Affect Neurocognitive Function in HIV-1 Infection: Balancing Viral Suppression against Neuronal Stress and Injury. *J Neuroimmune Pharmacol*, *16*(1), 90-112. https://doi.org/10.1007/s11481-019-09868-9

Yuan, N. Y., Maung, R., Xu, Z., Han, X., & Kaul, M. (2022). Arachidonic Acid Cascade and Eicosanoid Production Are Elevated While LTC4 Synthase Modulates the Lipidomics Profile in the Brain of the HIVgp120-Transgenic Mouse Model of NeuroHIV. *Cells*, *11*(13). https://doi.org/10.3390/cells11132123

Zhang, L. (2021). Method for voluntary oral administration of drugs in mice. *STAR Protoc*, *2*(1), 100330. https://doi.org/10.1016/j.xpro.2021.100330

Zhang, L., Lee, N. J., Nguyen, A. D., Enriquez, R. F., Riepler, S. J., Stehrer, B., Yulyaningsih, E., Lin, S., Shi, Y. C., Baldock, P. A., Herzog, H., & Sainsbury, A. (2010). Additive actions of the cannabinoid and neuropeptide Y systems on adiposity and lipid oxidation. *Diabetes Obes Metab*, *12*(7), 591-603. https://doi.org/10.1111/j.1463-1326.2009.01193.x